RSC Advances

PAPER

View Article Online
View Journal | View Issue

Cite this: *RSC Adv.*, 2024, **14**, 8652

Nanocellulose/wood ash-reinforced starch–chitosan hydrogel composites for soil conditioning and their impact on pea plant growth†

Dure Najaf Iqbal,*[a] Zaryab Tariq,[a] Boiz Philips,[a] Ayesha Sadiqa,[a] Muhammad Ahmad,[b] Khairia Mohammed Al-Ahmary,[c] Ijaz Ali[d] and Mahmood Ahmed *[b]

Hydrogels are 3-dimensional polymer networks capable of absorbing a large amount of water. Natural polymeric hydrogels are biodegradable, non-toxic and biocompatible. They can effectively retain nutrients for the plant and can be used as soil conditioners. This study uses a chemical cross-linking technique to synthesize starch and chitosan-based hydrogel using citric acid as a cross-linker. Additionally, hydrogel composites were developed by incorporating wood ash, nano-cellulose, and NPK (nitrogen–phosphorus–potassium) fertilizer as fillers to enhance their properties. The formulated hydrogel/hydrogel composite samples were characterized by FTIR spectroscopy, SEM analysis, X-ray diffraction and thermo-gravimetric analysis. The experiment results showed the chemical cross-linking among the polymeric chain and the semi-crystalline nature of the hydrogel/hydrogel composite samples. The swelling capacity of the hydrogel/hydrogel composite samples was 200–420% (in distilled water) and 104–220% (in saline medium) and demonstrated biodegradability within 110 days. The NPK reinforced hydrogel composite showed an excellent effect on the growth of pea plants (leaves count = 37, stem height = 20.2 cm), and could be effectively used as soil conditioners for agricultural applications. Considering the ability of hydrogel composites to reduce irrigation needs, enhance nutrient retention, and improve crop production, these novel hydrogel composites present an economically viable solution for sustainable agricultural practices.

Received 21st December 2023
Accepted 8th March 2024

DOI: 10.1039/d3ra08725e

rsc.li/rsc-advances

1 Introduction

There is growing demand for sustainable and environmentally friendly solutions that can improve crop output while reducing the negative environmental impact of contemporary agriculture practices. Leaching of nutrients, degradation of soil, and pollution of the environment are some of the critical problems frequently associated with conventional fertilizers and soil conditioners. For this reason, it is essential to develop new techniques that can successfully address these challenges and shift agricultural practices towards sustainability. Also, the consequences of climate change, defined by lower rainfall and increased drought and temperature changes, have further worsened these issues, resulting in decreasing crop yields due to water loss through evaporation and runoff. Thus, there is an urgent need for creative solutions that tackle these problems and advance sustainable farming methods.[1–3] Hydrogels are a palpable solution to this problem. Due to their hydrophilic nature and porous structure, hydrogels can retain a large amount of water. Natural polymers have been extensively used in formulating agricultural hydrogels in the past few decades. Bio-polymeric hydrogels are non-toxic, biodegradable and biocompatible. These hydrogels have proved to be an excellent soil conditioning material. Hydrogels have the potential to enhance the soil's water retention capacity, making them valuable for addressing water stress in crops cultivated in arid or drought-affected regions. Thanks to their excellent transport capabilities, these hydrogels enable the controlled and efficient delivery of fertilisers and other agrochemicals to plants. Additionally, they can be employed to regulate the soil's pH.[4,5]

Starch (SC) and chitosan (CS) are favorable polymers in creating agricultural hydrogels. Chitosan, derived from the abundant polysaccharide chitin, is a bio-polymer with potential anti-bacterial, anti-viral, and anti-fungal properties, capable of stimulating the defence systems of plants. On the other hand, starch is the predominant carbohydrate used for plant storage, existing in granular form in the chloroplasts of

[a]Department of Chemistry, The University of Lahore, Lahore, Pakistan. E-mail: dure.najaf@chem.uol.edu.pk
[b]Department of Chemistry, Division of Science and Technology, University of Education, Lahore-54770, Pakistan. E-mail: mahmood.ahmed@ue.edu.pk; mahmoodresearchscholar@gmail.com
[c]Department of Chemistry, College of Science, University of Jeddah, Jeddah, Saudi Arabia
[d]Centre for Applied Mathematics and Bioinformatics (CAMB), Gulf University for Science and Technology, Hawally, Kuwait

† Electronic supplementary information (ESI) available. See DOI: https://doi.org/10.1039/d3ra08725e

green leaves and the amyloplasts of seeds, tubers, and pulses.[6,7] The organic materials SC and CS are inexpensive, easily accessible, and sustainable. Their natural origin also renders them naturally non-toxic, biocompatible, and biodegradable, which is why they are frequently employed in the synthesis of hydrogel materials with possible agricultural applications. A more logical part of polymer matrices for uses in sustainable agriculture is being recognized as CS owing to its multifunctional role in plants. With the potential for widespread agricultural uses, SC is one of the most significant polysaccharides added to hydrogels.[8] SC- and CS-based hydrogels can be used in agricultural fields for soil amendment. They can enhance soil's water retention ability and help in the controlled delivery of nutrients, fertilisers, and other agrochemicals to plants. Hence, these hydrogels can economically increase the crop's quality and quantity.[9,10] Various methods for preparing SC and CS-based hydrogels with potential agricultural applications have been reported in the past few years. Alkaline hydrolysis has prepared superabsorbent hydrogel based on native cassava SC and polyacrylonitrile.[11] The graft polymerization technique synthesised pH-sensitive SC-polyacrylate hydrogel to deliver active materials to plants.[12] Hydrogel formulated by the gamma irradiation of SC and carboxymethyl cellulose (CMC) could efficiently enhance the water-holding ability.[13] Gamma irradiation technique has also been used to synthesize hydrogel based on nano-SC.[14] Chemical cross-linking of waxy corn SC with potato SC by succinic anhydride produced a hydrogel, a promising material for agricultural use.[15] Composite hydrogel based on SC and zeolite nano-particles was prepared, and the release of Zn ions from the hydrogel was investigated.[16] Methods for preparing CS-based agricultural hydrogels have also been reported for the controlled release of agrochemicals. Chemical cross-linking of CS (encapsulated with urea) using genipin has resulted in a microsphere formulation, which can be used as a soil conditioning agent.[17] A CS-based hydrogel was synthesised using EDTA and urea for the controlled release of urea and metal ions from the soil.[18] Hydrogel prepared by the chemical cross-linking of CS and SC using glutaraldehyde and glyoxal as cross-linking agents exhibits crucial agricultural applications.[19] SC and CS-based hydrogels have also been prepared for the controlled release of fertilisers using the ionotropic gelation technique.[20] Although these SC/CS synthesised hydrogels and hydrogel composites are biodegradable and have good swelling ability, they cannot deliver essential nutrients required for the growth and development of plants. Moreover, they do not have good mechanical strength. One way to make hydrogel matrices stronger is to add reinforcing fillers. To improve the characteristics of hydrogels based on starch and cellulose for agricultural purposes, scientists are exploring different approaches, such as chemical modifications, cross-linking techniques, and nanomaterials. Overcoming these challenges could lead to sustainable water management, better nutrient utilization, and less reliance on chemical fertilizers and pesticides in farming. New techniques have enabled the production of high-performance hydrogels using agricultural waste such as sugarcane bagasse and wood ash as cellulose sources.[21,22] In numerous developing nations, the practice of burning crop residues occurs on farms following harvest seasons, leading to the emission of substantial quantities of greenhouse gases such as CO_2, N_2O, and CH_4, as well as air pollutants like CO, NH_3, NO_x, SO_2, and volatile organic compounds, along with particulate matter. There is an immediate need for sustainable management of agricultural wastes. Most agricultural wastes typically comprise significant proportions of cellulose and hemicellulose.[23,24] Recent research has revealed that these mostly indigestible polysaccharides can be employed to produce superabsorbent hydrogels. These hydrogels are lightly cross-linked hydrophilic polymers that can absorb a substantial quantity of water or aqueous solution into their three-dimensional networks. In contrast to traditional hydrogels that utilize acrylate or acrylamide as their monomers, hydrogels based on cellulose exhibit superior biodegradability and biocompatibility.[25]

The objective of this work is to synthesize chemically cross-linked SC and CS-based hydrogel using citric acid as a cross-linker (Fig. 1). In addition the hydrogel composites were prepared by adding fillers such as nanocellulose (isolated from bagasse), wood ash (bamboo tree ash) and NPK fertiliser. Adding these fillers not only enhances the mechanical properties of the hydrogels but also supplies vital nutrients for the growth of plants. Using agricultural waste as a filler highlights the suggested hydrogel composites' environmentally benign and economically advantageous characteristics. This study is innovative because it takes a complete approach to improving the performance of SC/CS hydrogels for agricultural use. We aim to address agricultural sustainability and trash management by integrating fillers made from agricultural waste. Furthermore, applying a chemical cross-linking method allows for careful manipulation of the hydrogel's characteristics, guaranteeing excellent capacities to retain water and provide nutrients. The economical and environmentally friendly nanocellulose-based hydrogel composites derived from agricultural waste hold promise as future soil conditioners, providing a rationale for the current research design. The developed hydrogel composites were characterized using Fourier transform infrared spectroscopy (FTIR), scanning electron microscopy (SEM), X-ray diffraction (XRD), and thermal gravimetric analysis (TGA). The developed hydrogel composites were investigated regarding their degree of swelling, gel fraction and biodegradability. The impact of the hydrogel composites was also calculated on the growth of the pea plant (*Pisum sativum*).

2 Materials and methods

2.1 Materials

Sugarcane bagasse was obtained from the sugarcanes grown in the local farms of Punjab, Pakistan. Wood ash was obtained from the wood of bamboo trees found in Punjab, Pakistan. NPK fertiliser (15 : 15 : 15) was purchased from the Engro Fertilizer Limited, Pakistan. Sodium hypochlorite (10% available chlorine), sodium hydroxide, sulfuric acid (98%), corn starch,

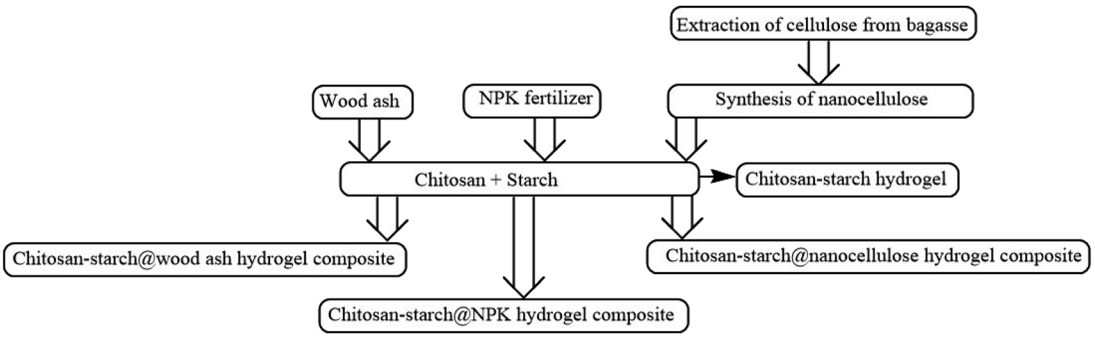

Fig. 1 Flowchart for the preparation of hydrogel/hydrogel composite.

chitosan (Mw = 310 000–375 000 g mol^{-1}, 87.8% deacetylation degree) and citric acid originated from Sigma Aldrich-USA and were purchased from the local supplier (Falcon Scientific, Lahore-Pakistan).

2.2 Extraction of cellulose

Cellulose was isolated from sugarcane bagasse by drying it in sunlight, cutting it into small pieces and then grinding it into powdered form (Retsch™ GM 200 Model Knife Mill, UK). To remove lignin, the powdered sugarcane bagasse was bleached with sodium hypochlorite (0.75% W/V) at 45 °C and then washed with distilled water. The neutral residue obtained was refluxed for 3.0 h with NaOH (150 mL, 17.5%) at 45 °C to remove hemicellulose. The residue was again washed with distilled water to neutralize it and finally dried for 2–3 days at room temperature.

2.3 Synthesis of nanocellulose

The isolated cellulose was hydrolysed with sulfuric acid, and cellulose to sulfuric acid was in a ratio of 1 : 25. The hydrolysis process was quenched by adding excess distilled water (10 folds/250 mL). The colloidal suspension produced was centrifuged for 30 min at 650 rpm, and then, to neutralize the suspension, it was dialysed for five days. Finally, the suspension obtained was sonicated for 10 min to homogenise the prepared nano-cellulose.

2.4 Preparation of hydrogel and composites

Hydrogel was prepared by dissolving 2 g of starch and 2 g of chitosan in citric acid (6% w/v, aqueous solution) and continuously stirring the reaction mixture for about 1.0 h at 80 °C. The hydrogel mixture was then allowed to stand for 15 min, casted into the Petri dish and then placed in the oven for 6 h at 100 °C to complete the cross-linking reaction. For hydrogel composites, 2 g of chitosan and 2 g of starch were dissolved in citric acid (6% aqueous solution) separately in three beakers. The mixtures were stirred continuously for 30 min, then 0.8 g of each filler (nanocellulose, wood ash and NPK fertiliser) was added into the reaction mixture in each beaker and stirring was continued for 30 min. The composite mixtures were then allowed to stand for 15 min, casted into Petri dishes, and placed in the oven at 100 °C to dry the hydrogel films and for cross-linking reaction. Sample codes of formulated hydrogel samples and their chemical composition are given in Table 1.

2.5 Characterisation

FTIR (Bruker Alpha Platinum ATR, USA) spectroscopic analysis of the sample was done to identify the structural changes that occur by the cross-linking reaction and to identify various functional groups present in the hydrogels. The FTIR spectrum of all the samples was recorded in the 7500–375 cm^{-1} range. Surface morphology and porosity of the hydrogel/hydrogel composite samples were investigated by SEM (Nova NanoSEM™, USA) analysis. ImageJ, an open-source image processing software was employed for porosity quantification. Using ImageJ's particle analysis tool, the total area occupied by pores in the hydrogel sample was measured. Concurrently, the total area of the hydrogel sample in the SEM images was quantified. Porosity was then calculated using the eqn (1). XRD (D2 PHASER XRD Analyzer, Bruker-USA) analysis of hydrogel samples was performed to determine the crystal structure of the hydrogel and composite hydrogel samples with a useable angular range of −3–160° 2-Theta. Degree of crystallinity of the hydrogel/hydrogel composite samples was also determined by dividing integrated area of all peaks in XRD diffractograms to the total integrated area under XRD peaks (eqn (2)). The thermal stability of the hydrogel/hydrogel composite samples was evaluated by TGA (SDT-Q600 TA Instruments, USA) analysis in a temperature range of 0–500 °C.

$$\text{Porosity}(\%) = \frac{\text{Pore area}}{\text{Total sample area}} \times 100 \quad (1)$$

$$\text{Degree of crystallinity} = \frac{\text{Area of all crystalline peaks}}{\text{Total area}} \times 100 \quad (2)$$

2.6 Degree of swelling

When hydrogel is immersed in water, it swells to some extent but does not dissolve in water. The gravimetric method determined hydrogel and composites' swelling degree or water absorption capacity. 0.2 g of each hydrogel composite sample was weighed (W_1) and soaked in distilled water and saline solution (0.9% NaCl). Then, samples were filtered out after intervals of 10 min, 15 min, 30 min, 60 min, 15 h and 24 h and

Table 1 Chemical composition and codes of formulated hydrogel/hydrogel composite samples

Sr. no.	Sample names and codes	Starch (g)	Chitosan (g)	Citric acid (6% w/v, mL)	Filler (g)
1	Starch-chitosan hydrogel (SCH-1)	2	2	100	—
2	Wood ash hydrogel composite (WAC-2)	2	2	100	Wood ash (0.8)
3	Nano-cellulose hydrogel composite (NCC-3)	2	2	100	Nano-cellulose (0.8)
4	NPK fertiliser hydrogel composite (FCC-4)	2	2	100	NPK fertiliser (0.8)

weighed each time (W_2) after removing extra water with the help of blotting paper. The swelling degree for each sample was calculated by using the following formula (3):

$$S(\%) = \frac{W_2 - W_1}{W_1} \times 100 \quad (3)$$

2.7 Gel fraction and weight loss in water

To determine the weight loss of hydrogel/hydrogel composite samples in water (W_s), the samples were dried for 4 h at 100 °C and weighed (W_0). The samples were then dipped in distilled water for 24 h. After that, the samples were dried for 4 h at 100 °C and weighed again (W_1). The calculation of weight loss of hydrogel/hydrogel composite samples in water (4) and the percentage gel fraction of hydrogel/hydrogel composite samples (5) can be calculated by the following formula:

$$W_s(\%) = \frac{W_0 - W_1}{W_0} \times 100 \quad (4)$$

$$\text{Gel fraction}(\%) = 100 - W_s \quad (5)$$

2.8 Biodegradability test and impact on growth of pea plant

A soil burial test was used to determine the biodegradability of the hydrogel samples. For this purpose, natural soil was taken from the University of Lahore-Pakistan campus, and the weighed amount (W_i) of sample hydrogels/composite was buried in the soil at a depth of 10 cm. The incubation temperature for the samples was maintained at 25 °C. The degraded samples of hydrogel and hydrogel composites were taken out of the soil at time intervals of 10, 30, 50, 70, 90, and 110 days and weighed each time (W_f). The degradation of the samples was then calculated by using the eqn (6):

$$\text{Degradation rate}(\%) = \frac{W_i - W_f}{W_f} \times 100 \quad (6)$$

The impact of the hydrogel/hydrogel composite samples on pea plant growth was also investigated. For this purpose, 5 pots filled with vegetable soil were taken. Hydrogel/composite samples were added in 4 pots. These pots were labelled with sample names (pot 2: hydrogel, pot 3: nanocellulose hydrogel composite, pot 4: wood ash hydrogel composite, and pot 5: NPK hydrogel composite). One of the pots (pot 1: control) was labelled as a control in which no hydrogel sample was added. Seeds of pea plants were sowed in each pot, and growth of the plants was noted after 10, 20 and 30 days.

3 Results and discussion

The chitosan–starch hydrogel and its composite with nanocellulose, bamboo wood ash and NPK fertiliser were successfully developed using citric acid as a cross-linker. The schematic layout of hydrogel and composites is presented in Fig. 2.

3.1 FTIR and XRD analysis

The neat starch showed its characteristic peaks at 3300 cm^{-1} (O–H stretch) and 1200 cm^{-1} (C–C stretch).[26] The spectrum of neat chitosan showed a broad peak from 3700–2900 cm^{-1} which indicate the N–H and O–H stretching vibrations. It also contain two prominent peaks at 1665 cm^{-1} (C=O stretch of amide-l) and 1577 cm^{-1} (N–H bending for amide II).[27] In contrast to proteins, which have more specialized secondary structures like alpha-helices or beta-sheets, chitosan's random coil structure can lead to a larger and less defined peak in the amide I region (around 1650–1700 cm^{-1}). Additionally, variables including molecular weight, the degree of deacetylation, and environmental circumstances might affect the position and strength of these bands. FTIR spectrum of citric acid showed its broad characteristic peaks between 3600–2500 cm^{-1} (O–H stretching). Two peaks observed at 1650 cm^{-1} and 1600 cm^{-1} arise from the C=O stretching vibrations.[28] The FTIR spectrum of neat starch, chitosan and citric acid are given in Fig. S1 (ESI).† FTIR spectroscopic analysis of the resultant material yields essential insights into the effectiveness and extent of crosslinking (Fig. 3). One standard method for improving chitosan-based hydrogels and films' mechanical strength and stability is to crosslink CS with citric acid. The primary process of this crosslinking is the creation of amide bonds between the citric acid carboxyl groups and the amine groups of CS. Because of its random coil shape, CS usually exhibits the amide band at 1700–1600 cm^{-1}. The amide band moves to a lower wavenumber (about 1570–1400 cm^{-1}) following crosslinking, signifying the creation of new amide bonds with citric acid. Two characteristic peaks were observed in 1585–1573 cm^{-1} and 1390–1380 cm^{-1} for all hydrogel/hydrogel composite samples. This confirms the crosslinking reaction between the amino group ($-NH_2$) of CS and the carboxyl group (–COOH) of citric acid. A characteristic peak for all hydrogel/hydrogel composite samples was observed in a region of 1725–1730 cm^{-1}, which is accompanied by a strong

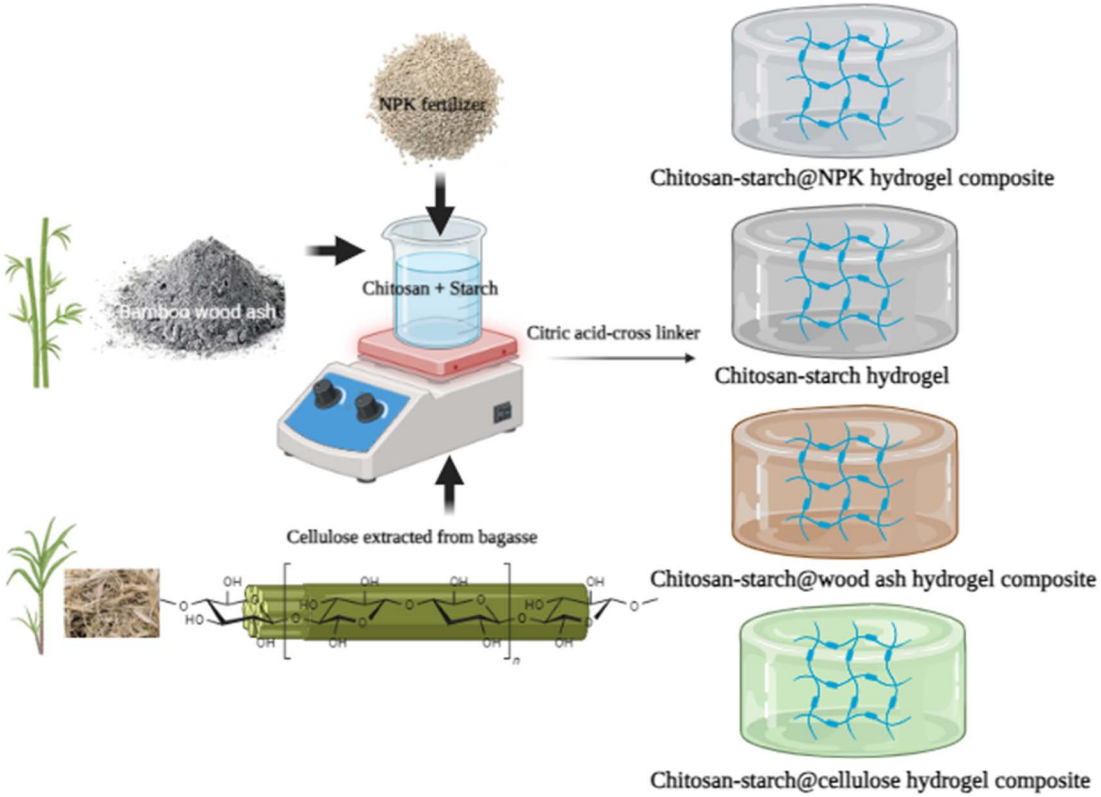

Fig. 2 Schematic layout for the preparation of chitosan–starch hydrogels and its composites.

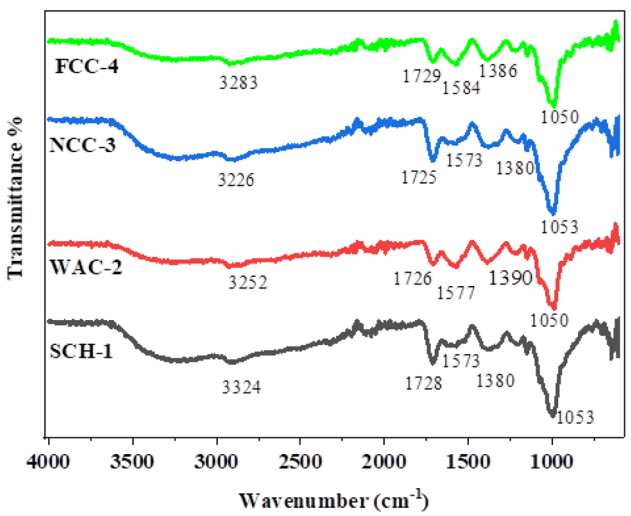

Fig. 3 FTIR spectra of hydrogel/hydrogel composites.

peak at 1050–1055 cm^{-1} (C–O stretch). This indicated the presence of an ester group in their chemical structure and confirmed the esterification reaction (chemical cross-linking) between the carboxyl group (–COOH) of citric acid and the hydroxyl group (–OH) of SC. Before crosslinking, citric acid peaks around 1650–1600 cm^{-1} due to its free carboxyl groups. After cross-linking, this peak diminishes or disappears as the carboxyl groups react with chitosan amine groups and the hydroxyl group (–OH) of starch.

X-ray diffraction analysis of fabricated hydrogel/hydrogel composite samples was also done to determine whether they were crystalline or amorphous. The results of the analysis are presented in Fig. 4. The characteristic peaks of the neat starch was observed at 13°, 15°, 16° and 20°.[29] Peaks for neat starch were observed at about 15° and 21°.[30] Citric acid showed sharp peaks at 14°, 18°, 19°, 23°, 25° and 28° which indicated its high degree of crystallinity.[31] The XRD graphs of neat starch, chitosan and citric acid are given in Fig. S2 (ESI).† The results indicated that all the hydrogel/hydrogel composite samples have a semi-crystalline structure. Several maxima in the XRD diffractograms revealed good structural order and high crystallinity in the hydrogel samples. XRD diffractogram of SCH-1 showed diffraction peaks at 14.1°, 21.6°, 23.6°, 28.2° and 37.3°. The degree of crystallinity for this hydrogel sample (SCH-1) was 42%. For WAC-2 hydrogel composite sample the peaks observed at 2θ value of 15.7°, 19.2°, 23.6°, 28.8°, 31.4°, 43° and 75.6°. The degree of crystallinity of WAC-2 was calculated to be 75%. NCC-3 hydrogel composite sample have shown almost 80% crystallinity, and the diffraction peaks were observed at 11.4°, 15.5°, 18.6°, 22.8°, 44.8°, 54°, 57°, 58° and 71°. XRD diffractogram of FCC-4 showed peaks at 14.7°, 19.6°, 23.2°, 29.1°, 43° and 62.7°. The degree of crystallinity for this particular hydrogel composite sample was 72%. The XRD analysis of all hydrogel/hydrogel composite samples showed slight displacement in the peaks of starch and chitosan which confirms the cross-linking reaction among polymeric chains. Some peaks of SC and CS have disappeared in the XRD curve of all samples, and

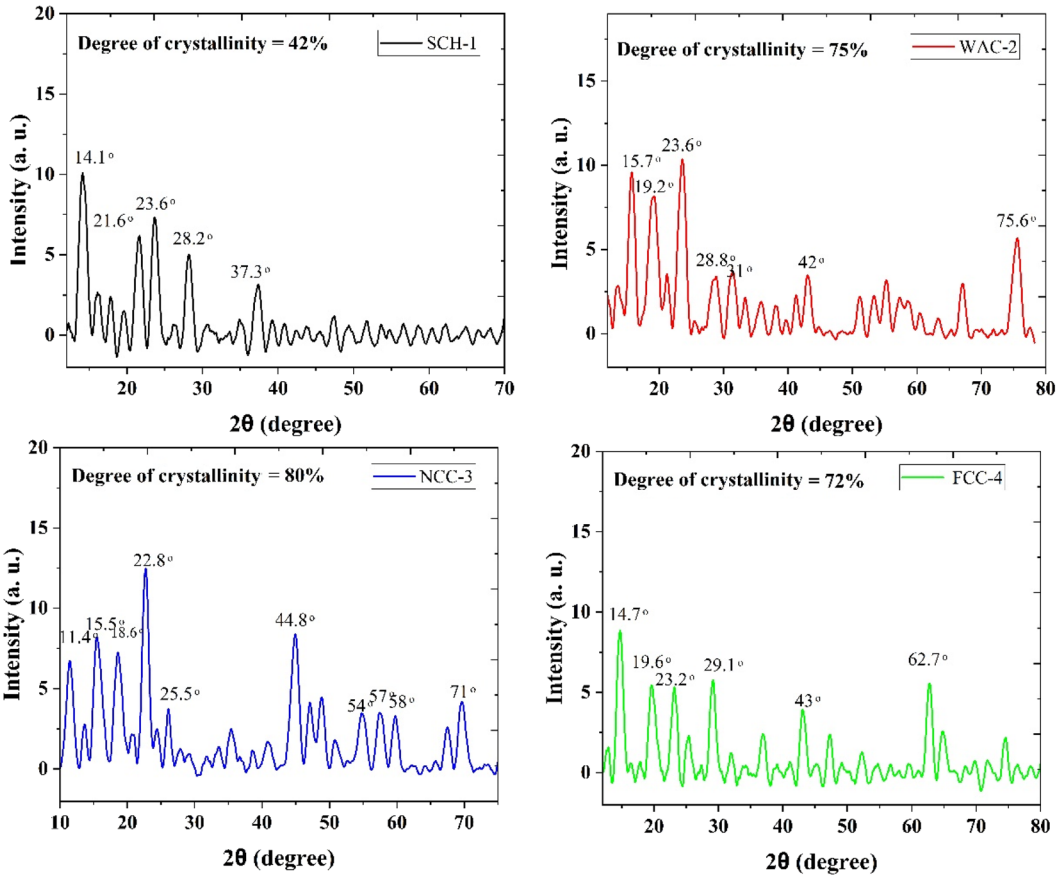

Fig. 4 XRD graphs of hydrogel/hydrogel composites.

some new peaks were observed due to a new structural order formed due to the cross-linking reaction and the addition of additives in the hydrogel. It was observed that more sharp peaks with high intensity are found in the diffractogram of the NCC-3 sample; hence, it has more crystallinity in its structure than all other samples. Nano-cellulose in the NCC-3 hydrogel composite sample has made the structure denser and more ordered in its crystalline form. The hydrogel composite samples WAC-2 and FCC-4 also showed good crystallinity and orderly arrangement in their crystalline structure. Crystallinity has decreased in SCH-1 due to its weak cross-linking. Thus, the order for the crystallinity of hydrogel/hydrogel composite samples is NCC-3 > WAC-2 > FCC-4 > SCH-1. It is cleared from the results of FTIR and XRD analysis that addition of fillers in the hydrogel have made the structure of hydrogel more compact by increasing the degree of cross linking and hereby result in the increase of the degree of crystallinity of the hydrogel composite samples. The hydrogel sample which does not contain any filler in it have less compact structure, low degree of cross linking and low crystallinity.

3.2 TGA and SEM analysis

TGA analysis was performed to estimate the thermal stability of formulated hydrogel/hydrogel composite samples. Thermal stability of hydrogel/hydrogel composite samples is a critical factor for the water retention. Temperature variations are common in agricultural settings. Various temperatures, including exposure to heat during the day and lower temperatures at night, must be tolerated by hydrogels used in agriculture. Under various climatic circumstances, thermal stability guarantees that the hydrogel will retain its structural integrity and functionality. In agriculture, hydrogels are frequently used to retain water and release fertilizers in a controlled manner. Thermal stability is crucial to prevent the hydrogel matrix from deteriorating or losing its efficacy when subjected to extended sun exposure. Agricultural hydrogels are often incorporated into the soil for extended periods. A hydrogel with good thermal stability will maintain its structural and chemical properties over time, ensuring long-term performance and sustained water conservation and nutrient release benefits. Weight loss of the hydrogel samples was determined with the increase in temperature. Thermograms of the prepared hydrogel/hydrogel composite samples are presented in Fig. 5. The weight loss up to 100 °C in all samples was due to the loss of water from them. The weight loss above 100 °C up to the first degradation stage was because of the decarboxylation and cleavage of carboxylate ion cross-linked bonds in the hydrogel/hydrogel composite samples. The thermogram curves revealed three stages of degradation for all samples. The first degradation stage for hydrogel/hydrogel composite samples starts between 170–190 °

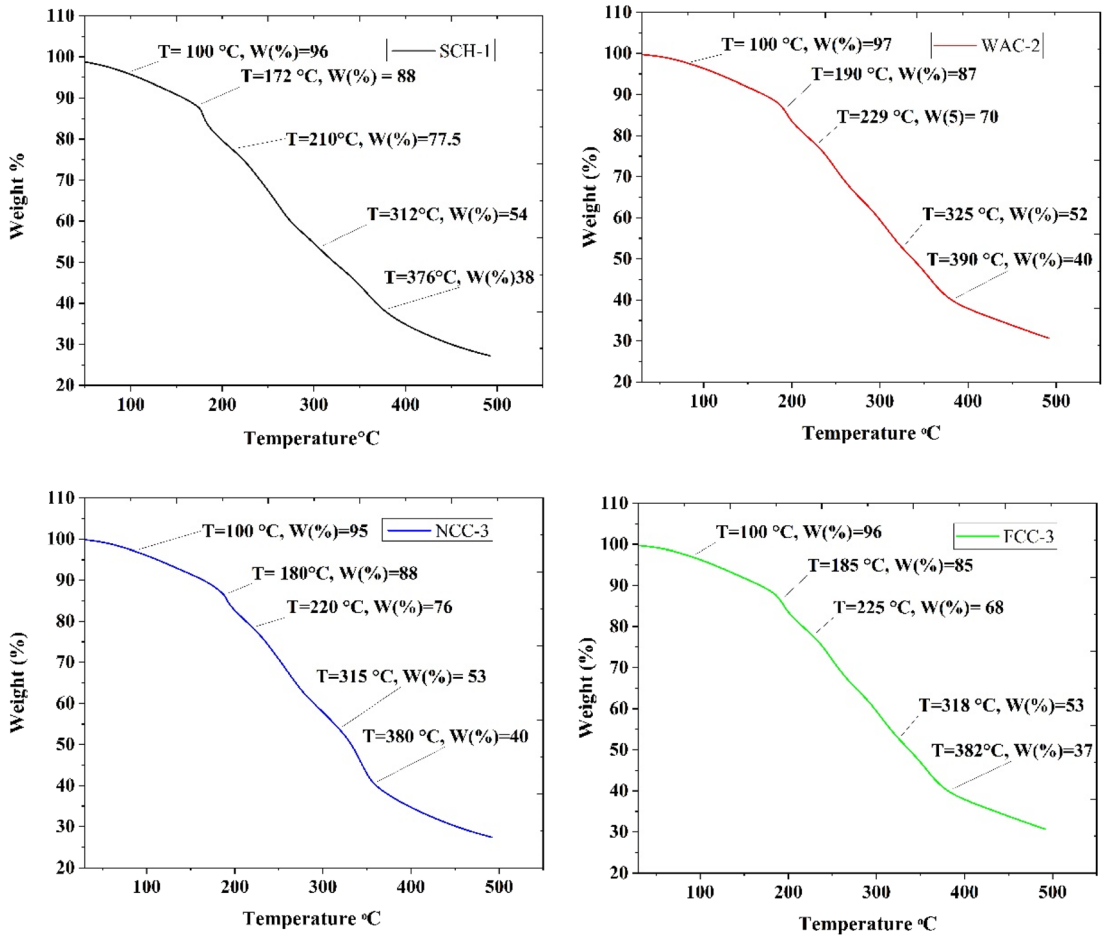

Fig. 5 TGA of hydrogel/hydrogel composites.

C, which indicates the cleavage of cross-linked ester bonds in them as the decomposition temperature for ester bonds is 150–210 °C.[32] The second degradation stage started at about 210–230 °C, where maximum weight loss occurred. This showed the degradation of starch present in them as the degradation temperature for the starch is 200–350 °C.[33] The third degradation step for all samples initiates at 310–325 °C, where degradation of chitosan is found in the hydrogel, as the decomposition temperature for chitosan is 300–390 °C.[34] Another transition in thermograms appeared at 375–385 °C, where the combustion of residual organic matter occurred, and the inorganic matter was left behind. For the SCH-1 hydrogel sample, the whole degradation process resulted in a weight loss of 50%. Cleavage of ester bond started at 172 °C, and weight loss occurred at 10%. Degradation of starch was initiated at 210 °C, and weight loss of 23.5% took place during this degradation step. Degradation of CS for SCH-1 started at 376 °C, and weight loss in this degradation step was 16%. Thermograms of the WAC-2 hydrogel composite sample revealed that the degradation process has resulted in a weight loss of 47%. The first degradation step, which involved the ester bond cleavage, started at 190 °C, and weight loss was found to be 17% during this degradation step. Pyrolysis of starch was initiated at about 229 °C and resulted in 18% weight loss. The decomposition of CS in this hydrogel composite sample was begun at 325 °C and resulted in a weight loss of 12%. The TGA curve for the NCC-3 hydrogel composite sample showed that a weight loss of 48% took place during the whole degradation process. Cleavage of cross-linked ester bonds was started at 185 °C, and weight loss during this stage was 12%. The thermal decomposition of starch began at 220 °C, and the weight loss of the sample during this degradation stage was 23%. Pyrolysis of CS was initiated at 315 °C, resulting in a weight loss of 13%. For the hydrogel composite sample FCC-4, degradation caused a weight loss of 48%. Ester bond decomposition was initiated at 185 °C and resulted in a weight loss of 17%. Pyrolysis of SC for FCC-4 was started at about 325 °C, and weight loss during the decomposition of SC was 15%. CS degradation was created at a temperature of 318 °C, and weight loss during this degradation step was 16%. It was observed that degradation of SCH-1 occurred at low temperatures, which indicated its lower thermal stability than all other hydrogel composite samples because it has weak cross-linking among its polymer chains. NCC-3 and FCC-4 showed comparatively better thermal stability than SCH-1. Thermal degradation of the WAC-2 occurred at a relatively higher temperature. It is the most stable thermally, with

chemical solid cross-linking among its polymeric chains. Thus, the overall decreasing order observed for the thermal stability of the hydrogel/hydrogel composite samples is WAC-2 > FCC-4 > NCC-3 > SCH-1.

The SEM images of formulated hydrogel/hydrogel composite samples are presented in Fig. 6. The results obtained by the SEM analysis of the prepared samples revealed that they have a porous structure. Hydrogel samples that do not contain any filler (SCH-1) have a smoother surface than other hydrogel composite samples. The addition of fillers in the hydrogel sample has roughed the surface. Porosity calculated for SCH-1, WAC-2, NCC-3 and FCC-4 is estimated to be 76%, 60%, 68% and 65%, respectively, and the pore size in samples decreases in the order of SCH-1 > NCC-3 > FCC-4 > WAC-2. Pore size was observed at its maximum in SCH-1, which is also attributed to its excellent water absorption capacity and weak cross-linking. Hydrogel composites have less pore size because adding additives has increased the cross-linking of the hydrogel, making the structure more compact and less porous. WAC-2 has the most compact design with a smaller pore size than the rest of the samples, which indicates potent cross-linking in this particular sample.

On the 100 μm scale bar, the porosity of hydrogel/hydrogel composite samples can be well visualized. The gels images are

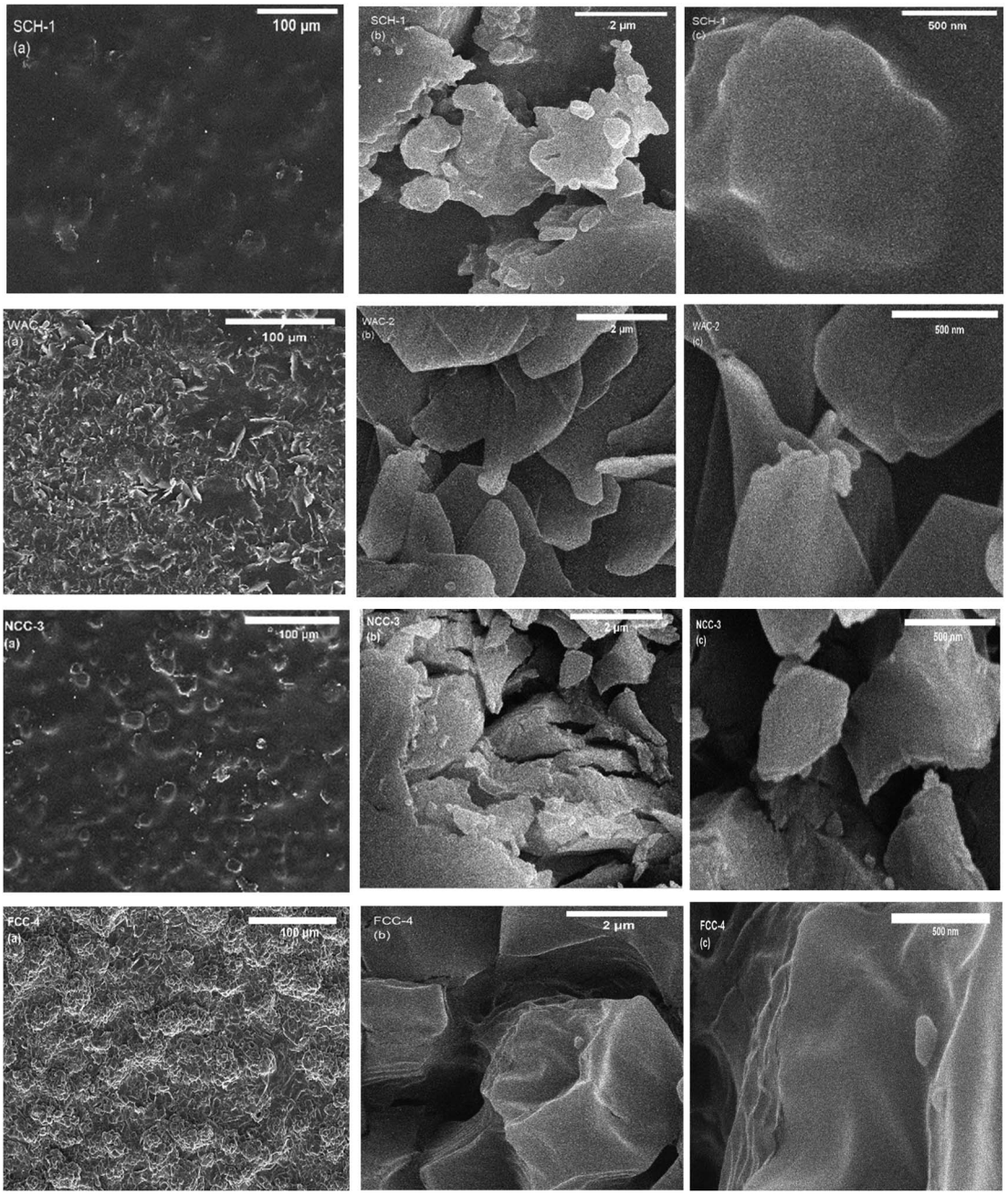

Fig. 6 SEM images of hydrogel/hydrogel composites.

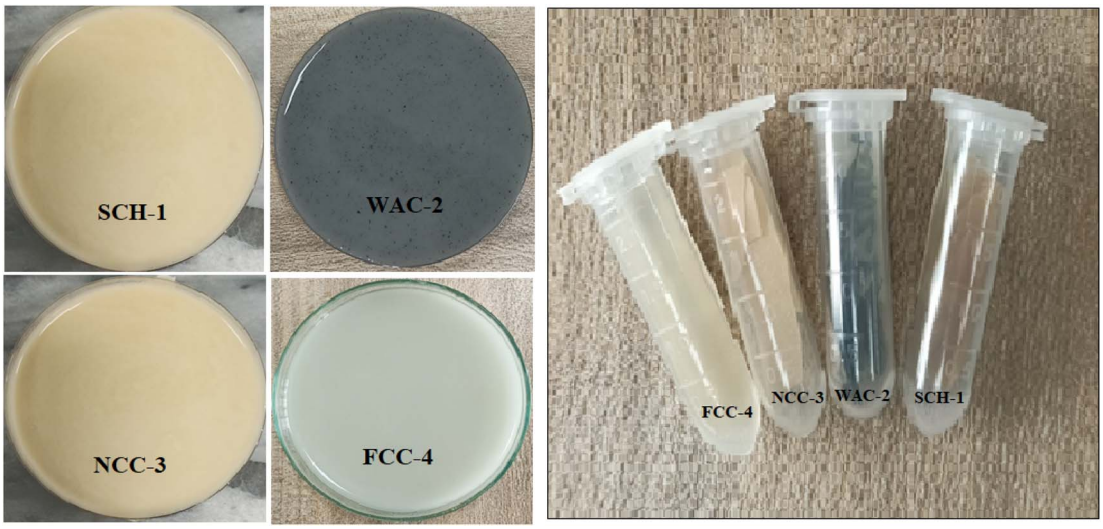

Fig. 7 Images of hydrogel/hydrogel composites in patri dishes and tubes.

shown in Fig. 7, in patri dishes and tubes. The degree of functionalization (DoF) has a bigger impact on the pores density, pores size, and porosity % in hydrogels that rely on functionalized groups to generate crosslinks than the polymer concentration, according to the results of SEM. Similar polymer concentrations in high-DoF hydrogels result in narrower pores than in low-DoF hydrogels.[35]

3.3 Swelling capacity

The water absorption capacity of the hydrogel/hydrogel composite samples was determined to evaluate their behavior in distilled water and saline solution. The results obtained are presented in Fig. 8a. It was observed that equilibrium swelling of all the samples was reached after 15 h. Water absorption in the NCC-3 hydrogel composite sample is found to be at its maximum. This is because nanocellulose provided more surface area for water absorption into the hydrogel. SCH-1 also showed good water absorption capacity because it has comparatively weak cross-linking between the polymer chains, which results in the availability of more free volume for the diffusion of water molecules. The lowest water absorption was observed in the hydrogel composite sample containing wood ash as a filler (WAC-2). This is due to stronger cross-linking in this hydrogel sample as it involves the interaction of inorganic ions in wood ash with the hydrogel. Hydrogel composite sample having NPK fertiliser (FCC-4) as a filler showed more water-holding ability than WAC-2 as it has comparatively less cross-linking among polymer chains than WAC-2. The same pattern for the water holding capacity of the samples was observed in saline solution (Fig. 8b). However, the water absorption capacity of the hydrogel/hydrogel composite samples was less in the salty medium than in distilled water. Thus, the overall decreasing order for the degree of swelling of samples is NCC-3 > SCH-1 > FCC-4 > WAC-2.

When considering the use of hydrogels for pea plants or other crops, it's important to note that excessive swelling may not always be beneficial. The goal is to provide adequate water retention for the plants without causing issues such as water-logging or impeding oxygen exchange in the root zone. The specific requirements for hydrogel swelling can vary based on factors like soil type, climate, and the water needs of pea plants. Some crops might require slower water release. By adjusting the crosslinking, hydrogels can swell gradually, preventing water-logging. Pea plants generally thrive in soil with good drainage, and overly swollen hydrogels might impede water movement and oxygen availability to the roots. Sandy soils may benefit from hydrogels with higher water retention capacity, while clayey soils may require hydrogels that improve aeration.

3.4 Gel fraction

A gel fraction test of the hydrogel/hydrogel composite samples was performed to estimate the degree of cross-linking in them, and it can be determined as the insoluble part of the hydrogel. Fig. 9a represents the results obtained from the test, which indicated that the WAC-2 sample shows the highest gel fraction (88%). This is because of the strong chemical cross-linking in this hydrogel composite. SCH-1, due to its weak cross-linking, showed the lowest gel fraction value (61%). The gel fractions for NCC-3 and FCC-4 samples were 65% and 75%, respectively.

3.5 Biodegradability

A soil burial test evaluated the biodegradability of the prepared hydrogel/hydrogel composite samples. The degradation rate of the samples is presented in Fig. 9b. As the hydrogel/hydrogel composite samples were buried in the regular soil, degradation of the hydrogel/composites took place by microorganisms present in the soil. Most of the mass of the hydrogel/hydrogel composite samples appeared to be lost within 30 days, and the samples showed a high degradation rate during the first 50 days, after which the degradation rate of the samples decreased. Complete hydrogel/hydrogel composite samples were degraded within 110 days. Hydrogel composite sample with wood ash as

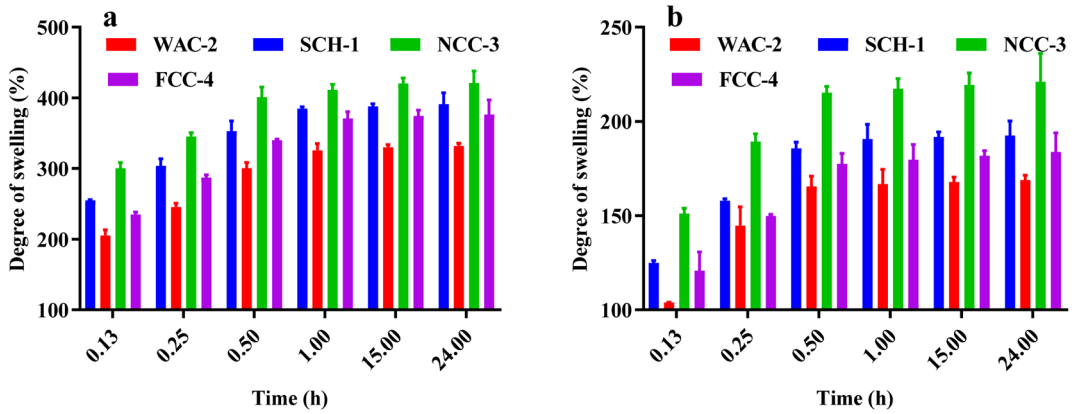

Fig. 8 Degree of swelling of hydrogel/hydrogel composites (a) in distilled water (b) in saline solution.

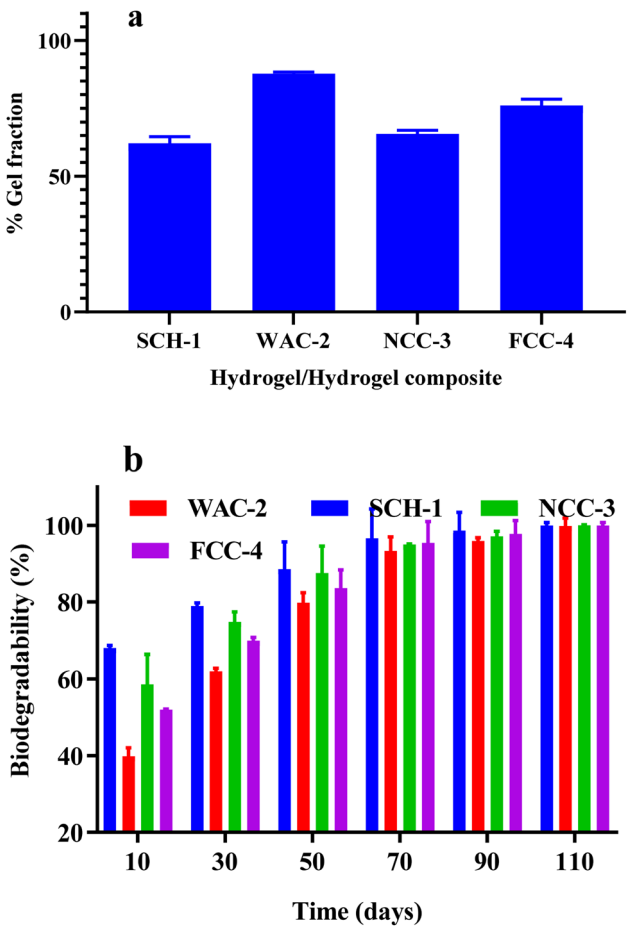

Fig. 9 Gel fraction of (a) hydrogel/hydrogel composites and (b) biodegradability (%).

a filler (WAC-2) showed a slow degradation rate among all the other samples. This is likely due to the strong cross-linking in this sample, which cannot be broken easily. Hydrogel composite samples NCC-3 and FCC-4 show intermediate degradation rates compared to other samples. At the same time, degradation occurs quickly in the SCH-1 hydrogel sample, which does not contain any filler. This hydrogel sample contains weak cross-linking and has a less compact structure, which the microorganisms can quickly degrade.

3.6 Impact of hydrogel composites on the growth of pea plant

The impact of the formulated hydrogel/hydrogel composite samples on pea plant growth (*Pisum sativum*) was also evaluated. The cultivated plants' stem height (Fig. 10a) and leaf count (Fig. 10b) were observed. Plant growth observed after 10, 20 and 30 days of harvesting seed is illustrated in Fig. 11. The control (without hydrogel samples) used for the experiment showed poor plant growth. The hydrogel sample SCH-1 plant growth was reasonable compared to the control plant. This is because hydrogel samples have increased the soil's water-holding capacity and thus enhanced the absorption of water by the plant. The plant grown in the presence of NCC-3 also showed good growth, more than SCH-1. The sample WAC-2, in which wood ash was used as a filler for hydrogel, showed excellent plant growth. This is because wood ash in the hydrogel contains essential nutrients required for the development of plants, and this hydrogel composite sample has effectively delivered those nutrients to the plant. The best growth of the plant was observed in a pot containing sample FCC-4, in which NPK fertiliser was used as a filler for hydrogel.

Both stem height and leaf count were at their maximum for this sample compared to others (Fig. 11). This showed the effective release of fertiliser from the formulated hydrogel composite. The fertiliser has provided essential nutrients (macronutrients) to the plant and thus enhanced its growth.

Utilized in agricultural settings, hydrogels serve as efficient reservoirs for retaining surplus irrigation water and plant nutrients. This enhances crops' efficient utilization of water and nutrients, leading to potential improvements in crop production.[24,36,37]

Previous studies may have investigated the application of CS-SC hydrogels in general soil conditioning or with different plant species. However, this study specifically targets pea plant growth, providing insights into the effectiveness of the hydrogel composite for a particular crop, explicitly targets pea plant growth and evaluates the effectiveness of the hydrogel

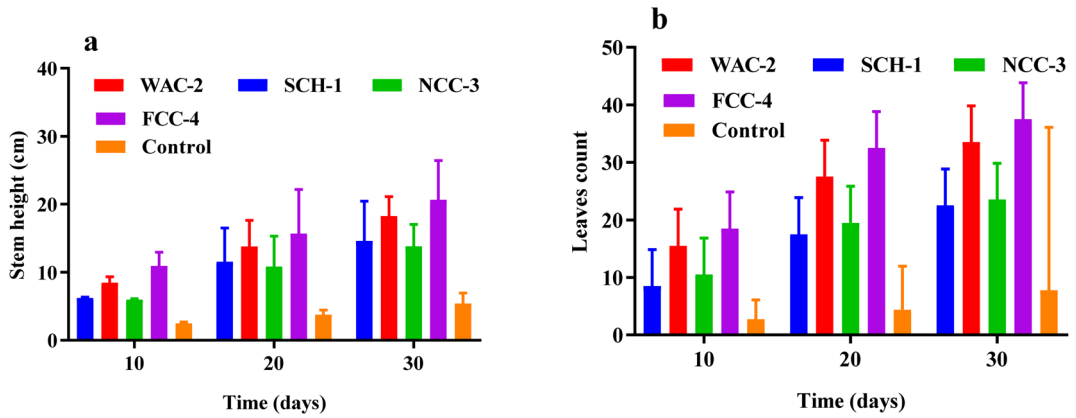

Fig. 10 Stem height (a) leaves count (b) of control (without hydrogel) and test plants (treated with hydrogel/hydrogel composites).

composite in promoting growth parameters such as plant height, leaf area, and biomass production.[8,38,39] The results of the pot experiments and growth parameter analysis suggest that the hydrogel composite effectively enhances pea plant growth. While other crosslinking agents, such as glutaraldehyde or glyoxal, might have been utilized in previous studies, the current research employs citric acid as a cross linker. This choice may offer advantages such as improved biocompatibility and reduced environmental impact. The current study incorporates fillers such as wood ash, nano-cellulose, and NPK fertilizer into the hydrogel composite to enhance its properties. This approach may differ from previous research. This study contributes to understanding the application of CS-SC hydrogels for a specific crop. It highlights the potential of incorporating fillers to improve the properties of the hydrogel composite.[20]

The strength of this study can be summarized as follows: the practical viability of employing hydrogels derived from

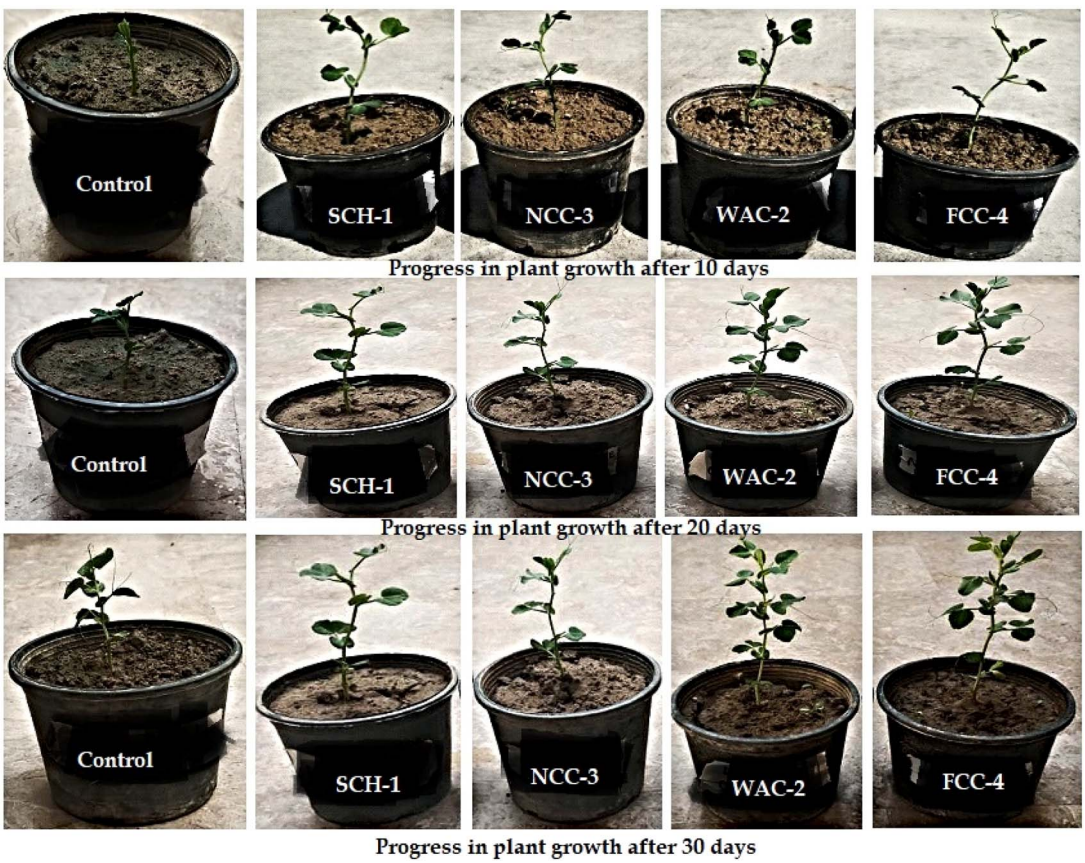

Fig. 11 Progress in pea plant growth treated with hydrogel/hydrogel composites.

agricultural waste in agriculture hinges on the successful optimization of net farm income (*i.e.*, gross farm income minus farm expenses). To achieve this objective, there should be a reduction in the inputs of irrigation water and fertilisers, coupled with an increase in crop yields. Using hydrogels derived from agricultural waste as soil amendments for enhancing agricultural production establishes a circular process focusing on the farmer. This process can maximize net farm income while minimizing the ecological footprint. Using nanocellulose-based hydrogels derived from agricultural waste involves renewable lignocellulosic biomass as raw materials, a shift away from unsustainable petroleum derivatives. This substitution represents a significant step toward mitigating greenhouse gas emissions. The environmental consequences of utilizing nanocellulose-based hydrogels in agriculture necessitate a comprehensive assessment throughout the product's entire life cycle, taking into account all processes during its production, application, and disposal. Each life cycle stage may involve natural or artificial inputs and the generation of environmentally harmful pollutants. For instance, transitioning from petroleum-derived raw materials to agricultural wastes has various impacts, including climate change, water scarcity, eutrophication, and biodiversity loss.[25] Before commercializing any new hydrogel products derived from agricultural waste, it is essential to comprehend their potential impacts on human health.

Moreover, there are limitations in the current study regarding environmental impact and human health that need to be addressed before considering commercialisation. The production of cellulose nanocrystals (CNCs) and nanofibrillated celluloses (NFCs) typically involves potentially hazardous chemicals such as strong acids, bases, and oxidants. Treating these chemicals modifies the surface charges of CNCs and NFCs, ultimately influencing their interactions with respiratory mucus and cells. Because body fluids contain substantial amounts of Na^+ and other cations with a charge-shielding effect, nanocellulose may easily aggregate, forming larger particles that are challenging to clear from the respiratory tract.

4 Conclusion

Eco-friendly hydrogel based on SC and CS has been successfully synthesised by a chemical cross-linking technique using citric acid as a cross-linker. Hydrogel composites have also been formulated using wood ash, nano-cellulose, and NPK fertiliser as fillers for hydrogel. Characterisation of formulated hydrogel/hydrogel composite samples by FTIR, SEM, XRD and TGA has confirmed the cross-linking reaction between SC, CS polymer and citric acid. Prepared samples are found to be semi-crystalline in nature. Nano-cellulose increases the density of the hydrogel and makes it more crystalline. NCC-3 (nano-cellulose hydrogel composite) sample has shown almost 80% crystallinity. Nanocellulose increases the water absorption capacity of the hydrogel (420%) by increasing the surface area available for absorption. Wood ash added to the hydrogel increased the degree of cross-linking in the hydrogel, resulting in more gel fraction (88%) in the wood ash hydrogel composite sample. Formulated hydrogel/hydrogel composite samples are biodegradable, and complete hydrogel samples are degraded within 110 days. All the samples are effective in increasing the growth of plants. Still, the best plant growth was observed with wood ash (leaves count = 34, stem height = 18.1 cm) and NPK hydrogel composite (leaves count = 37, stem height = 20.2 cm), which shows that they could effectively deliver essential nutrients to the plants. Hence, these composite samples can be used as a potential tool for agricultural applications. The use of nanotechnology in synthesising hydrogel is a promising strategy to enhance the desirable characteristics of the hydrogel. New methods should be devised to formulate hydrogel more economically. As modern chemical fertilisers are more toxic than organic fertilisers, the formulation of natural polymeric hydrogel composites based on traditional organic fertilisers should be encouraged to safely deliver water and nutrients to plants in a controlled way. Furthermore, the emphasis on natural polymeric hydrogel composites based on traditional organic fertilizers aligns with the need for safer alternatives to modern chemical fertilizers. This approach supports controlled nutrient delivery and contributes to environmental sustainability and a circular economy in agriculture. As this research moves forward, it is crucial to explore the life cycles of the developed hydrogel products in detail. Additionally, efforts should optimize cellulose wood ash sources, reagents, and methods to enhance the hydrogel's overall performance. The findings underscore the potential of these hydrogels/composites as a valuable tool in agriculture, providing a foundation for future studies and applications in environmentally conscious and sustainable farming practices.

Informed consent

This study was not performed on humans.

Data availability

This study did not report any data.

Conflicts of interest

The authors declare no conflict of interest.

Acknowledgements

The authors received no specific funding for this work.

References

1 S. Li, S. Hernandez and N. Salazar, *Sustain.*, 2023, **15**, 848.
2 J. Rockström, J. Williams, G. Daily, A. Noble, N. Matthews, L. Gordon, H. Wetterstrand, F. DeClerck, M. Shah and P. Steduto, *Ambio*, 2017, **46**, 4–17.
3 N. S. Singh, I. Mukherjee, S. K. Das and E. Varghese, *Bull. Environ. Contam. Toxicol.*, 2018, **100**, 553–559.
4 Z. Tariq, D. N. Iqbal, M. Rizwan, M. Ahmad, M. Faheem and M. Ahmed, *RSC Adv.*, 2023, **13**, 24731–24754.

5 C. J. Mate, I. Mukherjee and S. K. Das, *Environ. Monit. Assess.*, 2014, **186**, 7195–7202.
6 C. P. Jiménez-Gómez and J. A. Cecilia, *Molecules*, 2020, **25**, 3981.
7 H. Ismail, M. Irani and Z. Ahmad, *Int. J. Polym. Mater. Polym. Biomater.*, 2013, **62**, 411–420.
8 R. Michalik and I. Wandzik, *Polymers*, 2020, **12**, 2425.
9 M. Qamruzzaman, F. Ahmed and M. I. H. Mondal, *J. Polym. Environ.*, 2022, **30**, 19–50.
10 A. Berradi, F. Aziz, M. E. Achaby, N. Ouazzani and L. Mandi, *Polymers*, 2023, **15**, 2908.
11 L. Ekebafe, D. Ogbeifun and F. Okieimen, *Am. J. Poly. Sci.*, 2011, **1**, 6–11.
12 M. Sadeghi and F. Soleimani, *J. Biomater. Nanobiotechnol.*, 2012, **3**(2A), 310–314.
13 T. Fekete, J. Borsa, E. Takács and L. Wojnárovits, *Chem. Cent. J.*, 2017, **11**, 1–10.
14 I. Puspita, C. Winarti, A. Maddu and M. Kurniati, *IOP Conf. Ser. Earth Environ. Sci.*, 2023, **1267**, 012088.
15 V. Pathak and R. K. Ambrose, *J. Appl. Polym. Sci.*, 2020, **137**, 48523.
16 M. Yuvaraj and K. Subramanian, *J. Plant Nutr.*, 2018, **41**, 311–320.
17 M. R. Hussain, R. R. Devi and T. K. Maji, *Iran. Polym. J.*, 2012, **21**, 473–479.
18 K. Ravishankar and R. Dhamodharan, *React. Funct. Polym.*, 2020, **149**, 104517.
19 J. J. Perez and N. J. Francois, *Carbohydr. Polym.*, 2016, **148**, 134–142.
20 K. Supare and P. Mahanwar, *J. Polym. Environ.*, 2022, **30**, 2448–2461.
21 S. Li and G. Chen, *J. Cleaner Prod.*, 2020, **251**, 119669.
22 S. K. Das and G. K. Ghosh, *Biomass Convers. Biorefin.*, 2023, **13**, 12193–12204.
23 S. Li, G. Chen and A. Anandhi, *Energies*, 2018, **11**, 2951.
24 S. Li and G. Chen, *Environ. Dev. Sustain.*, 2020, **22**, 2703–2741.
25 D. M. Nascimento, Y. L. Nunes, M. C. Figueirêdo, H. M. de Azeredo, F. A. Aouada, J. P. Feitosa, M. F. Rosa and A. Dufresne, *Green Chem.*, 2018, **20**, 2428–2448.
26 R. Kumar, G. Ghoshal and M. Goyal, *J. Food Sci. Technol.*, 2021, **58**, 1227–1237.
27 C. Lustriane, F. M. Dwivany, V. Suendo and M. Reza, *J. Plant Biotechnol.*, 2018, **45**, 36–44.
28 K. Wilpiszewska, A. K. Antosik and M. Zdanowicz, *J. Polym. Environ.*, 2019, **27**, 1379–1387.
29 J. Guo, J. Wang, G. Zheng and X. Jiang, *J. Eng. Fibers Fabr.*, 2019, **14**, 1558925019865260.
30 S. B. Aziz, M. Hamsan, W. O. Karim, M. Kadir, M. Brza and O. G. Abdullah, *Biomolecules*, 2019, **9**, 267.
31 R. O. Toro, Doctoral Thesis, Universitat Politecnica De Valencia, 2015.
32 H. Peidayesh, Z. Ahmadi, H. A. Khonakdar, M. Abdouss and I. Chodák, *Polym. Adv. Technol.*, 2020, **31**, 1256–1269.
33 C. Wu, R. Sun, Q. Zhang and G. Zhong, *Carbohydr. Polym.*, 2020, **250**, 116985.
34 M. A. Diab, A. Z. El-Sonbati, M. M. Al-Halawany and D. M. D. Bader, *Open J. Polym. Chem.*, 2012, **2**, 14–20.
35 F. D. Martinez-Garcia, T. Fischer, A. Hayn, C. T. Mierke, J. K. Burgess and M. C. Harmsen, *Gels*, 2022, **8**, 535.
36 S. K. Das and G. K. Ghosh, *Biomass Convers. Biorefin.*, 2023, **13**, 13051–13063.
37 S. K. Das and G. K. Ghosh, *Energy*, 2022, **242**, 122977.
38 M. Salimi, B.-e. Channab, A. El Idrissi, M. Zahouily and E. Motamedi, *Carbohydr. Polym.*, 2023, **322**, 121326.
39 M. Mujtaba, K. M. Khawar, M. C. Camara, L. B. Carvalho, L. F. Fraceto, R. E. Morsi, M. Z. Elsabee, M. Kaya, J. Labidi and H. Ullah, *Int. J. Biol. Macromol.*, 2020, **154**, 683–697.